

## EXPERIMENTAL INSIGHTS INTO DYNAMIC BEHAVIOUR COMPOSITE LATTICE STRUCTURE

P. Jameekornkul\*, A. Panesar\*

\* IDEA Lab, Department of Aeronautics, Imperial College London, UK

### Abstract

This study investigates the dynamic response of composite lattice structures, a crucial aspect for design optimisation and real-world applications, particularly those requiring high energy absorption during impact events (e.g., crashworthiness). Employing drop-weight impact experiments, the research explores the influence of impact conditions and lattice design on deformation behaviour and energy absorption efficiency. By exploring the design options and design parameters, including density, material selection and the functionally grading strategy, the study provides a deeper understanding of how these factors affect lattice properties at higher strain rates. Additionally, the research characterizes the influence of fibre reinforcement in AM lattices to the dynamic response. The findings demonstrate that composite functionally graded metamaterials exhibit improved dynamic deformation behaviour compared to their uniform counterparts. Additionally, the work discussed the influence of strain rate on material properties. This knowledge paves the way for advancements in various engineering applications.

### Introduction

#### **Lattice structure**

Over the course of many years, metamaterials have been utilised for various engineering applications owing to its great mechanical properties e.g., honeycomb structures are valued for their high strength-to-weight ratio in lightweight sandwich panels [1], foams are employed for their energy absorption and damping capabilities in crash absorbers [2]. A recent development in lattice materials is the functionally graded structure, which allows for tailored mechanical properties and deformation modes in specific regions through controlled design parameters. Apart from volume fraction which is a primary design parameters, unit cell type [3] [4], size [5] and material [6] have shown to influence the lattice properties as well. Most of the influence of interest from the graded cellular materials have been shown as enhanced energy absorption [7] [8] and the highly specific mechanical properties through precise control [9].

The development of composite additive manufacturing (AM) has led to research on composite lattice structures, capitalising on the combined advantages of design and material properties. Composites offer similar benefits to lattice structures, including high strength-to-weight ratio and energy absorption. Several studies have explored composite lattice structures and demonstrated improved mechanical properties through toughening mechanisms [6]. For example, Chen and He [10] showcased enhanced specific energy absorption and relative modulus in auxetic lattices reinforced with short carbon fibers. Similarly, other studies [11] [12] investigated the benefits of fiber reinforcement in lattice structures through various designs, highlighting positive outcomes in terms of high strength and modulus. However, the addition of fiber reinforcement

introduces anisotropy and new deformation modes into the final product. This necessitates careful consideration during the design process to ensure optimal performance in specific applications. As noted by [12], the inherent anisotropy of these structures can lead to a reduction in modulus when compressed in the out-of-plane direction.

## **Dynamic behaviour of lattice**

While numerous studies have focused on lattice structures, the exploration of their dynamic performance remains limited compared to the well-established field of quasi-static behaviour. A review paper by [13] highlights the limitation of data on the high strain rate performance of AM lattice structures. Additionally, the effect of strain rate on the dynamic behaviour of lattice structures is still under debate. For instance, Harris et al. [14] observed that the specific energy absorption (SEA) of a hybrid honeycomb lattice reached its peak at an intermediate velocity, outperforming both quasi-static and high loading rates. However, a simulation by Li et al. [15] predicted that the SEA of a 316L gyroid lattice structure would be highest at the highest strain rate, with some experimental evidence supporting this claim. The limited understanding of the dynamic behaviour of composite lattice structures presents a significant knowledge gap that hinders their full potential in applications requiring high-impact energy absorption. Therefore, to address this gap, this study proposes to investigate the impact response of functionally graded composite AM lattices.

## **Aims**

This study aims to bridge the knowledge gap between the quasi-static behaviour of 3D lattice structures and their dynamic response under impact, particularly for energy-absorbing applications. We investigate functionally graded (FG) lattices with carbon fibre reinforcement subjected to drop-weight impact events. The work explores the influence of the FG lattice along with the comparison between composite and pure polymer materials. Our aim is to provide experimental insights into the dynamic behaviour of tailored lattice structures and ultimately achieve more controlled plastic deformation during impact through lattice design and material selection.

Therefore, our design of experiments involves exploring the effect of functionally graded density design. Additionally, we will explore the effect of integrating carbon fibre reinforcement compared to pure polymer lattices. The properties of composite lattices will also be characterised through microscopy. To quantify the mechanical performance of the lattices, the experimental data will be analysed for its strength and energy absorption, alongside with high-speed camera observation for qualitative assessment of the deformation behaviour. This comprehensive approach will provide valuable insights into the performance of AM composite and functionally graded lattice structures under impact, paving the way for their application in dynamic engineering scenarios.

## Methodology

### Design process

The Schwartz-P (SP) lattice was chosen as the representative stretching-dominated unit cell and the BCC lattice as the bending-dominated unit cell. The SP lattice is a surface-based Triply Periodic Minimal Surface (TPMS) structure, while the BCC lattice is a truss-based structure. The design of both lattices was generated by an in-house software using the method proposed in [16], where strut radius or offset thickness controls and tailors the density. A linear density gradient was implemented from the top surface to the bottom, achieving density variation between 0.2 and 0.8 in parallel to printing direction (or Z-axis, as shown in Figure 1). The overall dimensions of the lattice structures ( $20 \times 20 \times 20$  mm) with unit cell size of 5 mm and the global density ( $\rho = 0.5$ ) remained constant for all graded specimens.

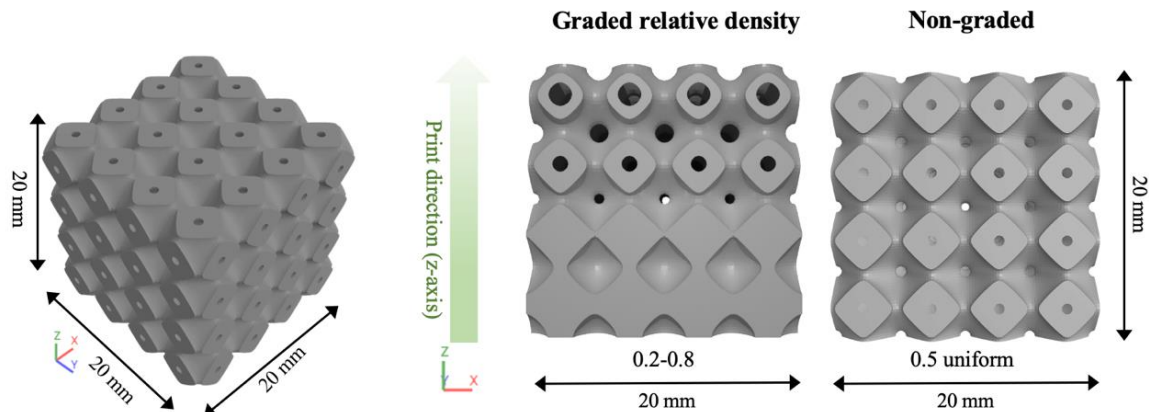


Figure 1: Lattice designs and dimensions

### Manufacturing process

Following the test matrix in Table 1, samples were fabricated using a Mark Two 3D printer by Markforged [17], which employs the material extrusion (ME) technique. Two materials were utilised: Nylon (PA6) and Onyx (CF/PA6). The latter allowed investigation of the influence of chopped carbon fibre reinforcement while maintaining a consistent matrix material (PA6). To minimise moisture absorption, filaments and printed samples were sealed and oven-dried for at least four hours before fabrication or testing. All designs were sliced using consistent settings within Eiger software. These settings included a layer height of 0.1 mm, no support structures, two wall layers, and a solid infill pattern. To prevent the moisture absorption effect, the filament was kept in the dry box during manufacturing and the built parts were kept in the oven at least 12 hours before impact testing.

## Experiment

The dynamic response of the samples was evaluated using a drop-weight impact test on an Instron drop-weight tower CEAST-9350 [18]. A 100 mm impactor weighted 26.10 kg was used to deliver an impact event. The impact energy applied is 15J giving impact velocity of 1.07 m/s and drop height of 59 mm. Upon impact and triggering the light gate sensor, the CEAST DAS 64K data acquisition (DAQ) system [18] recorded the contact force ( $F$ ) and time ( $t$ ) through the piezoelectric sensor on the 90kN load cell. A Phantom V641 high-speed camera [19] captured the deformation process for further analysis. Noted that the testing direction in this study is kept in parallel to the printing direction.

	Ungraded			Graded	Materials
<b><math>\rho</math> avg</b>	0.2	0.35	0.5	0.5	
	3	3	3	3	Onyx
	3	3	3	3	Nylon

Table 1: Test matrix shows number of repeats for each configuration.

To further understand the dynamic behaviour of the lattices, displacement ( $\delta$ ) and velocity ( $v$ ) at specific time point ( $t$ ) were calculated based on the non-uniform acceleration equation as a time-dependent function. The absorbed energy then calculated as the integral of the force-displacement curves.

The impact velocity ( $v_i$ ) was calculated using the principle of energy conservation, where the potential energy from the drop height equals the kinetic energy at impact:  $v_i = \sqrt{2gh}$ . The densification stage is not considered to contribute to the total absorbed energy [20]. This study defines the onset of densification as the point where the strain exceeds 0.5 strain as commonly considered as densification stage from previous studies [7] [20].

The additional parameters discussed in this study to further evaluate the dynamic response are primary peak force ( $F_{max}$ ) and maximum displacement ( $\delta_{max}$ ).  $F_{max}$  is the highest force during the first peak in force-displacement curve and the latter is the maximum displacement the impactor reaches during the impact event. The dynamic modulus value is derived from the strain range of 0.015-0.05 based on the dimensions described in Figure 1 and the material properties from [21]. The dynamic yield stress considered as the  $P_{max}/A_{nominal}$ .

## Results and Discussion

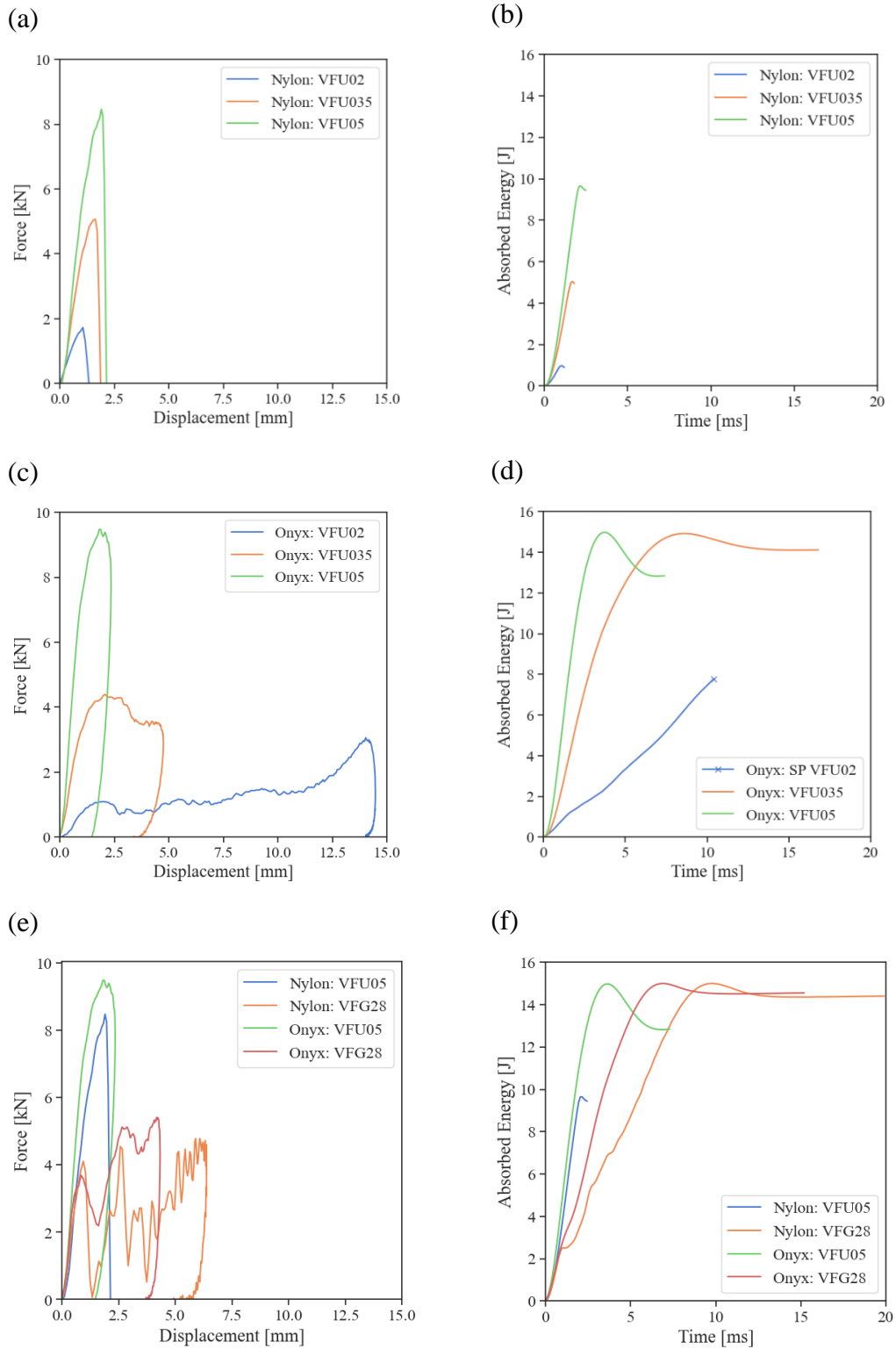


Figure 2: (a)(c)(e) Load-displacement curves (b)(d)(f) Absorbed energy-time curve, (a-b) Nylon material (c-d) Onyx material (e-f) Density-graded comparison

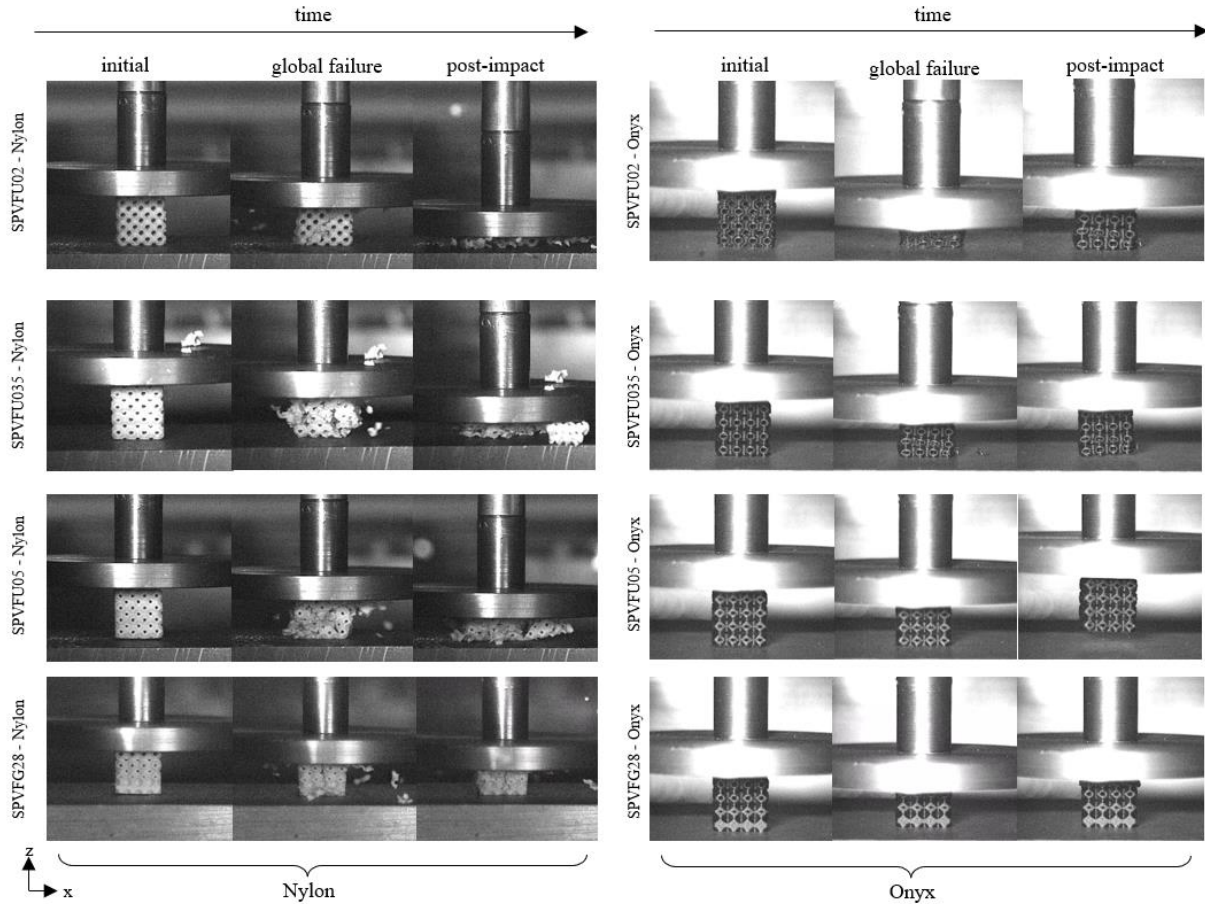


Figure 3: Deformation mechanism of uniform and density-graded lattices (Nylon and Onyx) recorded by Phantom high-speed camera

### Impact of Density, Material, and Fiber Reinforcement

For the Nylon uniform lattices, the varied density show the effect in force and energy profile shown in Figure 2a and Figure 2b respectively. As the lattice density increase, the maximum force and the maximum energy the lattice able to absorb also increase. This is owing to the stiffness of the part as proposed by Gibson and Ashby [22]. This trend also exhibited in the Onyx parts as well. However, it should be noted that all lattices in this study were subjected to a fixed impact energy of 15 J. While the Nylon uniform specimens couldn't fully absorb this energy, the Onyx uniform parts successfully did.

Lattices with carbon fibre reinforcement exhibited significantly higher absorbed energy by at least 4.1 J improvement compared to similar density ( $\rho_{avg} = 0.5$ ) Nylon lattices. This can be attributed to the larger maximum displacement achieved by the Onyx parts due to their progressive failure mode. In contrast, the Nylon parts experienced abrupt fractures, leading to a shorter impact duration and displacement. High-speed camera recordings supported these observations, revealing compaction in the Onyx parts compared to the catastrophic failure of the Nylon lattices (see Figure 3). The presence of random short carbon fibres in Onyx obstructs the global crack propagation, explaining the observed cracks and fractures in Nylon compared to the absence of such features in Onyx.

It is important to note that the lowest density Onyx part ( $\rho_{avg} = 0.2$ ) exceeded the 0.5 strain point, which is considered the onset densification. Energy absorption during densification is not typically considered. Therefore, while the energy profile for this part only reaches around 8 J in Figure 2d, it is still significantly higher than the pure polymer with the same density. For crashworthiness applications, Onyx parts are a preferable choice due to their ability to prolong failure and absorb higher impact energy compared to Nylon parts with similar design and weight. This advantage arises from the presence of carbon fibre reinforcement and the resulting progressive failure mode.

The dynamic yield strength for the experimental results was calculated by dividing the peak force by the nominal cross-sectional area of the lattice structure ( $20 \times 20 \text{ mm}$ ). The dynamic relative modulus was determined from the slope of the stress-strain curves within a specific strain range (0.015-0.05). The bulk modulus was obtained from a reference [21]. Both the dynamic yield strength and relative modulus were fitted to a power-law equation with minimal  $R^2 = 0.982$ . Compared to quasi-static data from previous research [7], the dynamic properties obtained in this study exhibit higher values. This can be attributed to the higher coefficient values observed in the power-law fits for the dynamic data. This trend aligns with the findings reported in the literature [23], where both yield strength and relative modulus are known to increase at higher strain rates. Interestingly, the exponent values in the yield strength plots are significantly lower than those in the quasi-static data. This suggests that the influence of density and the dynamic strain rate factor might be more pronounced for materials with higher density.

### Force Profiles and Energy Absorption in Graded Lattices

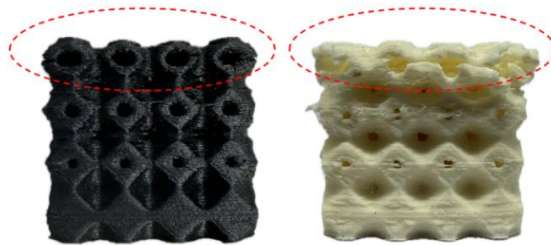


Figure 4: The comparison between post-impact density graded Onyx (left) and Nylon (right) specimens

Unlike uniform lattices, the force profiles of functionally graded lattices exhibit multiple peaks following the initial peak, as observed in Figure 2e. This phenomenon can be attributed to the progressive deformation sequence within the graded structure. The initial peak corresponds to the failure of the top contact layer, which has the lowest density due to the grading strategy. Subsequently, the impactor encounters denser layers with increasing stiffness, leading to further layer-by-layer failure until all impact energy is dissipated through plastic deformation or complete densification occurs. It's important to note that each subsequent layer has a higher density and, consequently, greater stiffness, contributing to the rise in multiple peak force values as the impactor progresses through the structure.

These multiple peaks translate to a larger energy absorption capacity compared to uniform parts with the same overall density. This improvement has been observed in both pure polymer and composite lattices. Even for composite structures that efficiently dissipate most of the applied energy, the force profile still exhibits multiple peaks, indicating successive failure and, therefore, significant potential for higher energy absorption capability compared to their uniform design in demanding applications.

It's noteworthy that the density of the top contact layer directly influences the first peak force and, consequently, the dynamic yield strength of the graded part. This is evident in the force profiles (Figure 2e) and the post-impact parts (Figure 4). The lower peak force can be beneficial in reducing the impact force experienced by passengers within a vehicle during a crash event. Therefore, graded lattices are ideal for applications where high overall energy absorption and minimising the initial contact force are crucial, even if it comes at the cost of potential initial damage to the crash absorber itself.

### **Conclusion**

The drop-weight impact tests revealed a correlation between density and mechanical properties, consistent with a power-law relationship. However, the dynamic response exhibited higher relative strength and modulus compared to quasi-static behavior. This can be attributed to strain rate sensitivity and inertia effects during impact. The deformation modes observed in lattices with linearly varying densities displayed progressive failure similar to quasi-static conditions. This progressive failure mechanism contributes to improved energy absorption during impact.

Furthermore, this study provides clear evidence that the integration of carbon fibers significantly improves the deformation mechanism. Unlike unreinforced materials that experience abrupt fracture, carbon fiber composites undergo compaction with minimal visible cracks. This enhanced ability to absorb impact energy highlights the potential of these composite lattice structures for crashworthiness applications. The research effectively bridges the knowledge gap between quasi-static compressive behavior and dynamic response. Additionally, it provides valuable insights into utilising composite AM for improved crashworthiness in various engineering fields.



## Reference

- [1] H. Mohammadi *et al.*, ‘An insight from nature: honeycomb pattern in advanced structural design for impact energy absorption’, *J. Mater. Res. Technol.*, vol. 22, pp. 2862–2887, Jan. 2023, doi: 10.1016/j.jmrt.2022.12.063.
- [2] Y. Duan *et al.*, ‘Dynamic response of additively manufactured graded foams’, *Compos. Part B Eng.*, vol. 183, p. 107630, Feb. 2020, doi: 10.1016/j.compositesb.2019.107630.
- [3] J. Kadkhodapour *et al.*, ‘Failure mechanisms of additively manufactured porous biomaterials: Effects of porosity and type of unit cell’, *J. Mech. Behav. Biomed. Mater.*, vol. 50, pp. 180–191, Oct. 2015, doi: 10.1016/j.jmbbm.2015.06.012.
- [4] O. Alketan, R. Rowshan, and R. Abu Al-Rub, ‘Topology-Mechanical Property Relationship of 3D Printed Strut, Skeletal, and Sheet Based Periodic Metallic Cellular Materials’, *Addit. Manuf.*, vol. 19, pp. 167–183, Jan. 2018, doi: 10.1016/j.addma.2017.12.006.
- [5] X. Yang *et al.*, ‘Effect of volume fraction and unit cell size on manufacturability and compressive behaviors of Ni-Ti triply periodic minimal surface lattices’, *Addit. Manuf.*, vol. 54, p. 102737, Jun. 2022, doi: 10.1016/j.addma.2022.102737.
- [6] S. Aghajani, C. Wu, Q. Li, and J. Fang, ‘Additively manufactured composite lattices: A state-of-the-art review on fabrications, architectures, constituent materials, mechanical properties, and future directions’, *Thin-Walled Struct.*, vol. 197, p. 111539, Apr. 2024, doi: 10.1016/j.tws.2023.111539.
- [7] J. Plocher and A. Panesar, ‘Effect of density and unit cell size grading on the stiffness and energy absorption of short fibre-reinforced functionally graded lattice structures’, *Addit. Manuf.*, vol. 33, p. 101171, May 2020, doi: 10.1016/j.addma.2020.101171.
- [8] H. Yin, W. Zhang, L. Zhu, F. Meng, J. Liu, and G. Wen, ‘Review on lattice structures for energy absorption properties’, *Compos. Struct.*, vol. 304, p. 116397, Jan. 2023, doi: 10.1016/j.compstruct.2022.116397.
- [9] Y. Li *et al.*, ‘A Review on Functionally Graded Materials and Structures via Additive Manufacturing: From Multi-Scale Design to Versatile Functional Properties’, *Adv. Mater. Technol.*, vol. 5, no. 6, p. 1900981, 2020, doi: 10.1002/admt.201900981.
- [10] Y. Chen and Q. He, ‘3D-printed short carbon fibre reinforced perforated structures with negative Poisson’s ratios: Mechanisms and design’, *Compos. Struct.*, vol. 236, p. 111859, Mar. 2020, doi: 10.1016/j.compstruct.2020.111859.
- [11] C. Hu, J. Dong, J. Luo, Q.-H. Qin, and G. Sun, ‘3D printing of chiral carbon fiber reinforced polylactic acid composites with negative Poisson’s ratios’, *Compos. Part B Eng.*, vol. 201, p. 108400, Nov. 2020, doi: 10.1016/j.compositesb.2020.108400.
- [12] J. J. Andrew, H. Alhashmi, A. Schiffer, S. Kumar, and V. S. Deshpande, ‘Energy absorption and self-sensing performance of 3D printed CF/PEEK cellular composites’, *Mater. Des.*, vol. 208, p. 109863, Oct. 2021, doi: 10.1016/j.matdes.2021.109863.
- [13] A. E. Medvedev, T. Maconachie, M. Leary, M. Qian, and M. Brandt, ‘Perspectives on additive manufacturing for dynamic impact applications’, *Mater. Des.*, vol. 221, p. 110963, Sep. 2022, doi: 10.1016/j.matdes.2022.110963.
- [14] J. A. Harris, R. E. Winter, and G. J. McShane, ‘Impact response of additively manufactured metallic hybrid lattice materials’, *Int. J. Impact Eng.*, vol. 104, pp. 177–191, Jun. 2017, doi: 10.1016/j.ijimpeng.2017.02.007.
- [15] X. Li, L. Xiao, and W. Song, ‘Compressive behavior of selective laser melting printed Gyroid structures under dynamic loading’, *Addit. Manuf.*, vol. 46, p. 102054, Oct. 2021, doi: 10.1016/j.addma.2021.102054.

- [16] A. Panesar, M. Abdi, D. Hickman, and I. Ashcroft, 'Strategies for functionally graded lattice structures derived using topology optimisation for Additive Manufacturing', *Addit. Manuf.*, vol. 19, pp. 81–94, Jan. 2018, doi: 10.1016/j.addma.2017.11.008.
- [17] 'Carbon Fiber Composite 3D Printer: Markforged Mark Two'. Accessed: Jun. 11, 2024. [Online]. Available: <https://markforged.com/3d-printers/mark-two>
- [18] Instron, 'Accessories for CEAST Impact Systems'. Accessed: Jun. 18, 2024. [Online]. Available: <https://www.instron.com/en-us/-/media/literature-library/products/2013/03/accessories-for-ceast-impact-systems.pdf>
- [19] 'Phantom v641 - Vision Research | Adept Turnkey'. Accessed: Jun. 18, 2024. [Online]. Available: <https://www.adept.net.au/cameras/visionresearch/Phantomv641.shtml>
- [20] Q. M. Li, I. Magkiriadis, and J. J. Harrigan, 'Compressive Strain at the Onset of Densification of Cellular Solids', *J. Cell. Plast.*, vol. 42, no. 5, Art. no. 5, Sep. 2006, doi: 10.1177/0021955X06063519.
- [21] Z. Eren, C. A. Burnett, D. Wright, and Z. Kazancı, 'Compressive characterisation of 3D printed composite materials using continuous fibre fabrication', *Int. J. Lightweight Mater. Manuf.*, vol. 6, no. 4, pp. 494–507, Dec. 2023, doi: 10.1016/j.ijlmm.2023.05.002.
- [22] L. J. Gibson and M. F. Ashby, *Cellular Solids: Structure and Properties*. Cambridge University Press, 1997.
- [23] X. Li, L. Xiao, and W. Song, 'Compressive behavior of selective laser melting printed Gyroid structures under dynamic loading', *Addit. Manuf.*, vol. 46, p. 102054, Oct. 2021, doi: 10.1016/j.addma.2021.102054.